AAPS PharmSciTech (© 2018)
DOI: 10.1208/s12249-018-1030-3

Research Article

Development of a Topical 48-H Release Formulation as an Anti-scarring Treatment for Deep Partial-Thickness Burns

Rossella Dorati,[1,2] Jorge L. Medina,[1] Patrick P. DeLuca,[3] and Kai P. Leung[1,4]

Received 18 December 2017; accepted 23 April 2018

Abstract. The purpose of this study was to develop pirfenidone (PF) ointment formulations for a dose finding study in the prophylactic treatment of deep partial-thickness burns in a mouse model. A preformulation study was performed to evaluate the solubility of PF in buffers and different solvents and its stability. Three different formulations containing 1, 3.5, and 6.5% *w*/*w* PF were prepared and optimized for their composition for testing in mice. Optimized formulations showed promising *in vitro* release profiles, in which 20–45% of PF was released in the first 7 h and 70–90% released within 48 h. The rheological properties of the ointment remained stable throughout storage at 25 ± 2°C/60% RH. Animal studies showed treatments of burn wounds during the inflammatory stage of wound healing with PF ointments at different drug concentrations had no adverse effects on reepithelization. Moreover, 6.5% PF ointment (F3) reduced the expression of pro-inflammatory cytokines IL-12p70 and TNFα. This study suggests that hydrocarbon base ointment could be a promising dosage form for topical delivery of PF in treatment of deep partial-thickness burns.

KEY WORDS: pirfenidone; ointment formulations; burn treatment; deep partial-thickness burn; mice.

INTRODUCTION

The purposes of this research were to develop a topical formulation of pirfenidone (PF), an anti-fibrotic drug, and to evaluate topical delivery of the drug, to treat skin fibrosis caused by burn injury in a mouse burn model. Hypertrophic scarring, an aberrant form of skin fibrosis with excessive accumulation of collagen, develops in as much as half or more of deep partial-thickness burn wounds. Unlike full-thickness burns, deep partial-thickness burn wounds retain some dermal elements including keratinocyte stem cells and fibroblasts that provide regenerative capacity. However, exuberant activation of these cells can drive hypertrophic scar formation (1,2). Hypertrophic scars are often raised, red, and hard and may cause abnormal sensations and such pathological scarring can lead to severe functional impairment, psychological morbidity, and costly long-term healthcare (3).

Treatments of hypertrophic scars are only minimally effective (1,4–6) due to the difficulty of reorganizing collagen into its normal architecture. Current treatments to facilitate the process, including laser and scar revision operations, have limited success at best. Therefore, prophylaxis is a viable strategy against the deposition of collagen in a scarred architecture. This may be accomplished by applying prophylactic treatments early in the course of burn care, in the inflammatory phase, and extending them into the proliferation and remodeling phases of wound healing.

In this context, the selection and development of a proper dosage form play a beneficial role in validating the prophylaxis strategy. Developing a dosage form for treatment of burn scars includes specific safety concerns associated with required excipients, sterility requirement to prevent infection, delivery of active agent in an effective way, diversity of scars in terms of depth size and location, and specific patient compliance such as low tolerance to selected excipients, frequency of treatment and severity of pain during application.

PF, an FDA-approved anti-fibrotic drug indicated for treatment of idiopathic pulmonary fibrosis, is a small molecular weight (185 g/mol) pyridinone with the chemical name of pyridine (5-methyl-1-phenyl-2-(1H)-pyridinone). PF has proven anti-fibrotic/anti-inflammatory activity in organs in addition to the lung, such as the liver, heart, and kidney in animal models (7) and clinical trials (8–10). However, its

Electronic supplementary material The online version of this article (https://doi.org/10.1208/s12249-018-1030-3) contains supplementary material, which is available to authorized users.

[1] Dental and Craniofacial Trauma Research and Tissue Regeneration, US Army Institute of Surgical Research, 3650 Chambers Pass, JBSA Fort Sam, Houston, Texas 78234-7767, USA.
[2] Department of Drug Sciences, University of Pavia, V.le Taramelli 12, 27100, Pavia, Italy.
[3] College of Pharmacy, University of Kentucky, Lexington, Kentucky, USA.
[4] To whom correspondence should be addressed. (e–mail: kai.p.leung.civ@mail.mil)

Published online: 11 May 2018

treatment effect on reducing skin fibrosis and diminishing excessive scarring has not been fully studied (11).

Our *in vitro* studies showed that PF was effective in lessening transforming growth factor (TGF)-β1 effects on the differentiation of human dermal fibroblasts into fibrotic myofibroblasts, the cell phenotype that promotes wound fibrosis (scarring) (12). PF decreased fibroblast proliferation and migration as well as lessened the pro-fibrotic phenotype of myofibroblasts with reduced production of α-smooth muscle actin, stress fibers, and collagen (12). Our *in vitro* data on TGF-β1-stimulated differentiation of dermal fibroblasts to myofibroblasts (12) and those that were reported in other systems (13) suggested that PF inhibits mitogen-activated protein kinase (MAPK) pathways downstream of receptors for growth factors, cytokines, and stress sensors as its mechanisms of action. MAPK pathways have been implicated in promoting myofibroblast differentiation signaled by TGF-β in rat myofibroblasts (14).

To test PF effectiveness as an anti-fibrotic agent, topical delivery in a mouse deep partial-thickness burn model at early post-wounding times was the selected strategy.

As indicated in regulatory assessment report for Esbriet® (EMA/CHMP/115147/2011), PF is stable in the solid state under stress conditions. The photostability study demonstrated good stability of PF in the solid state when exposed to visible light; however, degradation has been observed under visible light exposure of PF in solution.

Considering the poor stability of PF in solution and improved stability of PF in reduced content of water in hydrocarbon base formulations (less than 20% water), hydrocarbon base ointment was selected for the present study. Moreover, compared with cream, gel, and liquid dosage forms, hydrocarbon base ointment provides thicker consistency, increased stability, maintenance of wound moisture, and longer contact time of the drug at the treatment site.

The purpose of the present work was to develop PF ointment formulations for a dose finding study in the treatment of deep partial-thickness burns in a mouse burn model. Three different formulations containing 1, 3.5, and 6.5% *w/w* PF were prepared, and the selection of the maximum dose used in the present study was based on information available in the literature. Only a few papers have been published about using topical formulations containing PF as anti-fibrotic agent for treating skin diseases. Some of the findings related to treatment doses are summarized below.

Rodríguez-Castellanos et al. studied a topical formulation based on gel containing 8% of PF to treat localized scleroderma in 12 patients. Patients were instructed to apply 8% pirfenidone gel three times daily for 6 months using the standard fingertip unit (0.5 g for an area of 100 to 120 cm^2). Formulations presented good safety and tolerability (15). Giri SN et al. evaluated the effectiveness of pirfenidone ointment against thermoplasty-induced acute foreleg lameness in a double-blind study and against acute and chronic lameness of musculoskeletal origin in an open multi-centered field trial. A 10% pirfenidone or placebo ointment was topically applied on horses starting 24 h after the thermoplasty three times daily for 7 days (16).

In the present study, ointment formulations (1, 3.5, and 6.5 *w/w* PF) were optimized to attain PF sustained release for 48 h achieving cumulative 50–60% of drug released in 24 h and > 80% in 48 h.

MATERIALS AND METHODS

Materials

PF was obtained from AK Scientific Union City, CA (99% HPLC, Mw 185.22 g/mol). Vaseline® (ointment base), mineral oil (MO), and fetal bovine serum (FBS) were purchased from Sigma Aldrich (USA). Polyethylene glycol (PEG, Mw 400 Da) and Benzyl Alcohol (BnOH) were obtained from Spectrum (USA). Oxoid™ Maximum Recovery Diluent (MRD) and acetonitrile (MeCN, HPLC grade) were obtained from ThemoFisher Scientific (USA). All chemicals used were of analytical grade.

Methods

Preformulation Study

Pirfenidone Solubility.

Pirfenidone Solubility in Buffers

PF solubility in phosphate buffers at pH values 5.0, 6.0, and 7.4 was evaluated at refrigerated conditions, 22 or 34°C. Fifty milligrams of PF was placed in a scintillation vial and 1 ml of buffer was added. The resulting suspensions were maintained at above temperatures for 1 h under magnetic stirring. The suspensions were then filtered through 13-mm-

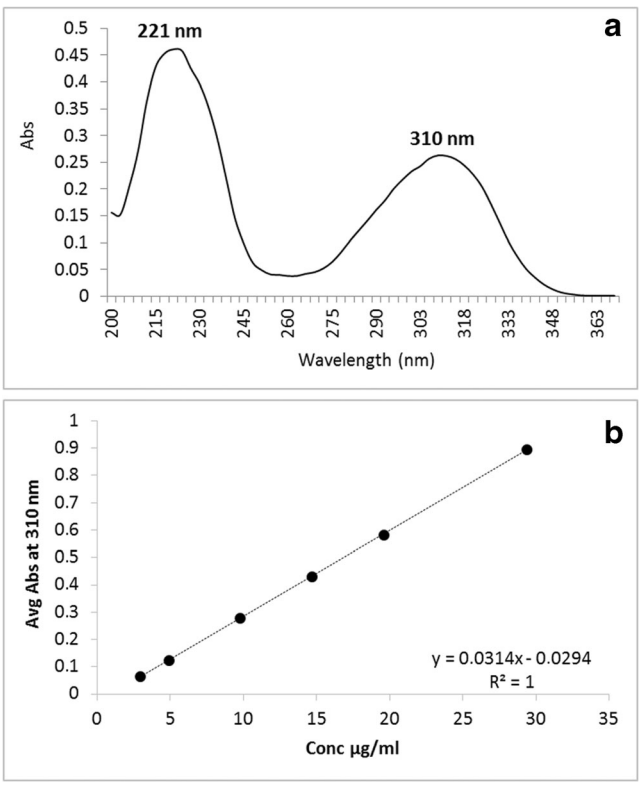

Fig. 1. **a** The UV spectrum of the standard solution of PF in MeOH (10 µg/ml) and **b** the absorbance curve of PF solutions of different PF concentrations (3–30 µg/ml) measured at 310 nm

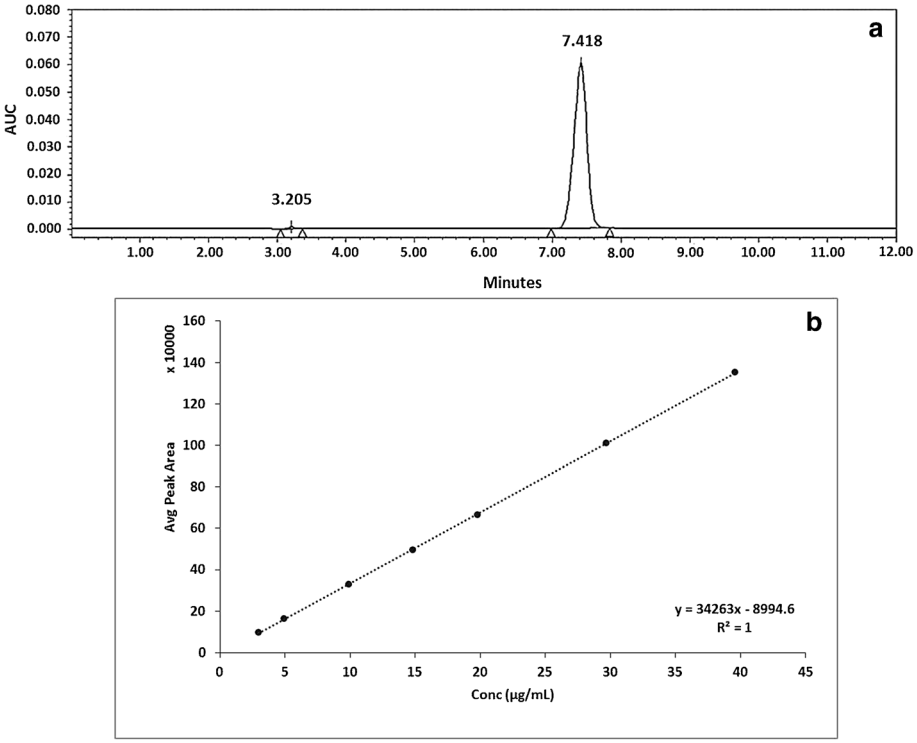

Fig. 2. **a** The HPLC assay chromatogram of pirfenidone in MeOH (10 μg/ml) showing PF peaked at 7.418 min. **b** A calibration curve of PF in MeOH (3–30 μg/ml) showing a linear relationship between PF concentrations and peak absorbance area measured at 310 nm

diameter PVDF syringe filters (Acrodisc® syringe filters, 0.22 μm) to separate the suspended PF from the dissolved drug. The filters were preliminarily validated (by HPLC) to check for any possible drug adsorption or other forms of interaction on the filter membrane. The solutions were analyzed by UV-vis spectrophotometry (described below) upon proper dilution. All experiments were performed in triplicate.

Solubility Test of PF in Water, Methanol, and Ethanol

PF solubility in water, methanol (MeOH), and 95% ethanol (EtOH) was assayed at 50–60 mg/ml. The test was performed by placing PF powder into a vial and by adding 1 ml of solvent. The system was kept at 22°C under magnetic stirring for a time sufficiently long to reach equilibrium. Samples were prepared and analyzed as described above.

Pirfenidone Stability in Solution

Stability of PF in liquid state was investigated at refrigerated temperature, 22 and 34°C, to assess the best conditions for the storage and *in vitro* studies. Briefly, a weighed amount of PF was dissolved in H_2O, PEG, and MeOH, and the solutions were incubated and protected from light at above temperatures for 28 days. Photostability study was conducted by exposing PF solutions to visible light at the same conditions described above. Samples were withdrawn at predetermined time points and submitted to high-pressure liquid chromatography (HPLC) analysis upon proper dilution. All experiments were performed in duplicate.

Method of Analysis (HPLC and UV).

To quantify PF in the ointment formulations, HPLC and UV methods were used.

Table I. Formulation of PF Ointment Formulations

Formulations	Pirfenidone (%)	Ointment base (%)	Mineral oil (%)	Polyethylene glycol (%)	Benzyl alcohol (%)
F1	1.0	78	20	–	1
F2	3.5	70	20	5	1
F3	6.5	90	2.5	–	1

Batch size, 50 g

Table II. Physical Evaluation of PF Ointment Containing 1, 3.5, and 6.5% of PF (Mean ± Sd, $n = 3$)

Formulations	Color	Clarity	Homogeneity	pH	Extrudability (%)	Viscosity (Pa·s)	Drug content (%)
F1	White	+++	+++	7.9	83.0 ± 1.9	3381	98.5 ± 0.9
F2	Off white	+++	+++	7.8	83.0 ± 1.5	5777	98.9 ± 1.0
F3	Off white	+++	+++	8.5	79.9 ± 0.6	9502	101 ± 2.7

Key: +++ excellent, ++ very good, + good, − unsatisfactory

UV Method

The spectrophotometric system consists of a single-beam Genesys 10 UV (Thermo Electron Corporation, USA) having two matched 10 mm quartz cells with 1-cm light path.

PF was determined from a standard calibration curve prepared starting from a stock solution containing 1 mg/ml PF in 5 ml MeOH (Fig. 1). The stock solution was diluted in a volumetric flask with deionized water (DIW) to obtain solutions of 3, 5, 10, 15, 20, 25, and 30 μg/ml of PF. Each standard solution was analyzed in triplicate and each point of the calibration curve is the average of the three analyses (17,18).

HPLC Method

PF was analyzed by reversed-phase Water® HPLC system (Water Corporation, USA) with an Inertsil ODS-2column (5 μm, 150 Å, 250 × 4.60 mm, Supelco). The mobile phase consisted of a mixture of KH_2PO4 buffer (0.02 M, pH 2.5 adjusted with H_3PO4) and MeCN at a ratio of 65:35 and was filtered through a nylon filter membrane (pore size 0.45 μm) before use. The flow rate of the mobile phase was 1.0 ml/min. The column temperature was maintained at 22°C (SSI 505LC column oven) and the wavelength was set at 310 nm for monitoring. The injection volume was 20 μl and the run time was 12 min. PF was determined from a standard calibration curve prepared starting from a stock solution containing 1 mg/ml PF in 5 ml MeOH (Fig. 2) in the same manner as that for the UV technique (18,19).

Preparation of Ointment Formulations

PF powder was first wetted with mineral oil used as a levigating agent; then, the wetted powder was incorporated mechanically into the ointment base. PEG and BnOH were included as co-solvent and preservative agent, respectively. The components were mixed until a uniform formulation was attained. Table I summarizes the composition of the ointment formulations.

To avoid component interactions during terminal sterilization, each ingredient was sterilized individually using an appropriate procedure. The ointment base was sterilized by dry heat at 160°C for 2 h, while mineral oil and PEG were steam sterilized by autoclaving at 121°C for 15 min. BnOH was sterilized by filtration using a 13-mm-diameter PVDF syringe filter (Acrodisc® syringe filters, 0.22 μm). The aseptically prepared formulations were filled under laminar air flow into multiple-dose aluminum tubes (approx. 10 g each tube) and stored at 25 ± 2°C/60% RH until further use.

Quality Control Procedures

Physical Examination. The prepared PF ointment formulations were inspected visually for their color, clarity, and homogeneity. After the ointments were filled in the aluminum tubes, they were evaluated again for color, clarity, and homogeneity by visual inspection. They were also evaluated for the presence of any aggregates or phase separation.

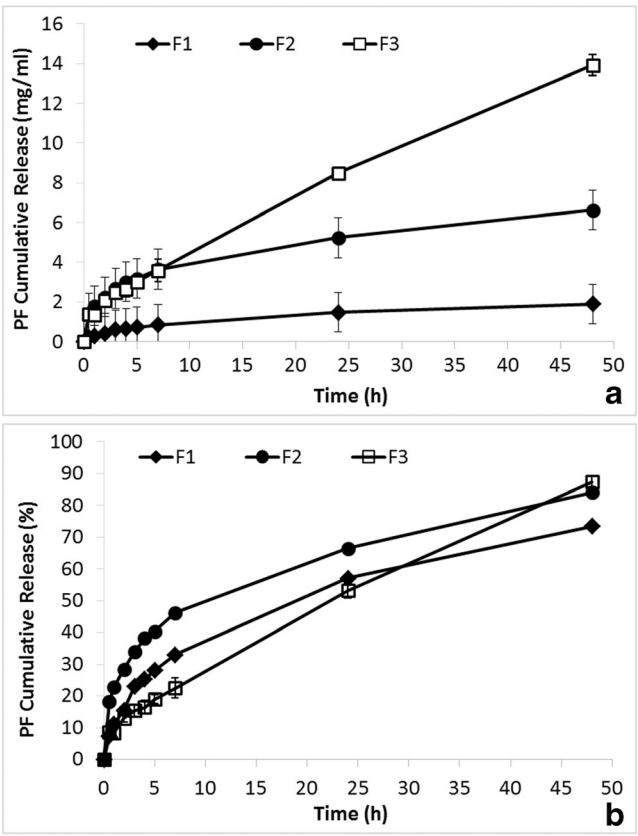

Fig. 3. *In vitro* release studies of the PF ointment formulations, F1, F2, and F3. The mg/ml PF cumulative release (**a**) and % PF cumulative release (**b**) *vs.* incubation time. The results were normalized to 250 mg of ointment. *In vitro* release was performed in PBS, pH 6.8, and at 34°C ($n = 3$)

Table III. Drug Release Kinetics Parameters of PF Ointment Formulations

Models*	Parameters**	Formulations		
		F1	F2	F3
Zero-order	R^2	0.902	0.890	0.994
$Q_t = Q_0 + k_0 \times t$	K_0	0.122	0.520	0.504
First-order	R^2	0.646	0.715	0.865
Log $Q_t = \log Q_0 + k_1 \times t$ / 2.303	K_1	0.215	0.133	0.377
Higuchi	R^2	0.988	0.984	0.979
$Q = K_H \times t_{1/2}$	K_H	0.322	1.38	1.36

*Q_t is the amount of drug released at time t; Q_0 is the initial amount of drug; K_0, K_1, and K_H are, respectively, the zero-order, first-order, and Higuchi's kinetic constants
**R^2 correlation coefficient

Determination of Drug Content. The PF ointments were tested for the drug content uniformity. A weighed quantity of formulation was transferred to a vial containing 50 ml of MeOH and allowed to stand for 3 h to ensure complete solubility of the drug. Following filtration with a nylon membrane, the solution was suitably diluted in H_2O and the PF content determined by HPLC at 310 nm.

In Vitro Diffusion Studies (Kinetic Study). A Franz diffusion cell (Vertical Diffusion Cell from Hanson Research Corporation, effective diffusion volume cell 7 ml) was used for the drug release studies. The test ointment (200 mg) was applied onto the surface of cellulose acetate membrane (GE Healthcare Life Sciences 0.45 μm, diameter 25 mm), which was clamped between the donor and the receptor chambers of the diffusion cell. The receptor chamber, which contained the freshly prepared phosphate-buffered saline (PBS) at pH 6.8, was continuously stirred by a magnetic stirrer and maintained at 34°C (20). Samples (1.0 ml aliquots) were collected at various time intervals and analyzed after appropriate dilutions in H_2O for drug content by HPLC at 310 nm. After each sample was taken, the volume was replaced with 1 ml of fresh buffer.

In Vitro Drug Release Kinetics. To examine the drug release kinetics and mechanism, the cumulative release data were fitted to models representing the zero-order, first-order, and Higuchi equation (21).

Rheological Characterization. Rheological measurements were performed using a Rheometrics Dynamic Analyzer RDA2. All experiments were conducted at room temperature (22°C) and using a parallel plate geometry. An adhesive backed sand paper was applied to the parallel plates to prevent sample slippage at the sample-plate interface.

Rheological characterization for each sample included four steps performed in sequence: time sweep (at strain, γ_0, of 0.1% and frequency, ω, of 1 Hz) was conducted for 10 min to allow the formulation to relax the stress accumulated during the sample loading. It was followed by strain sweep test (γ_0 0.1–50% and ω 1 Hz). A second strain sweep test was carried out for 10 min before the steady-shear test by varying shear rate from 0.02 to 100 s^{-1}.

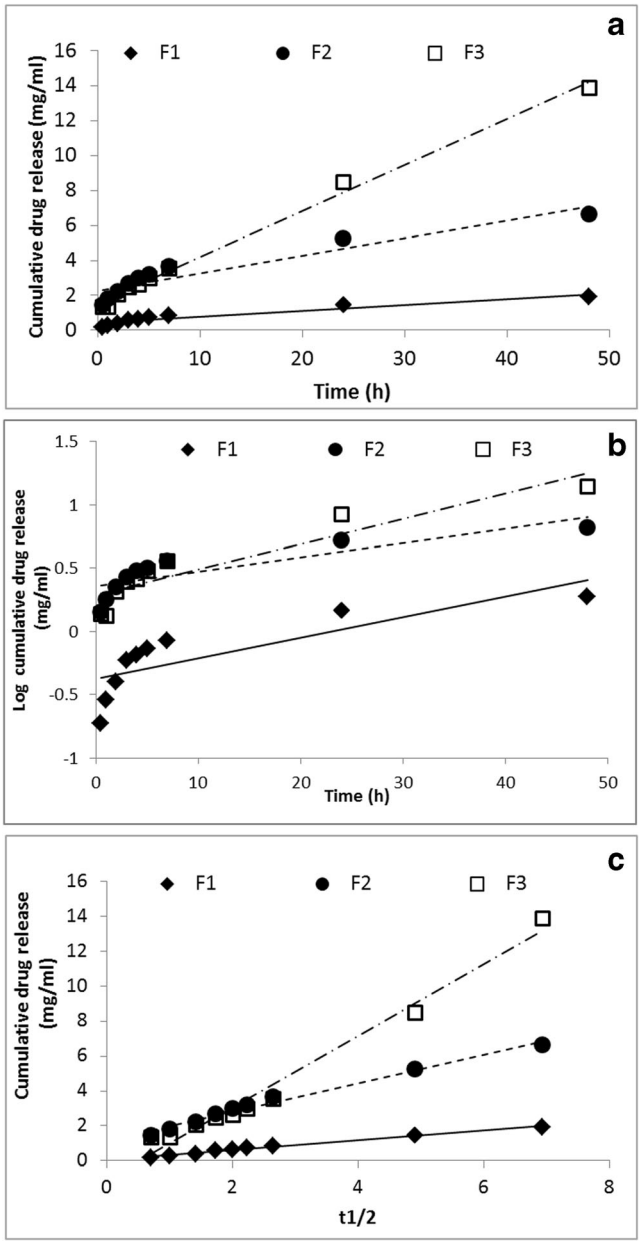

Fig. 4. PF drug release from the ointment formulations (F1, F2, and F3) with time. **a** Cumulative drug release (mg/ml) in linear time scale; **b** log cumulative drug release (mg/ml) plotted against linear time scale; **c** cumulative drug release (mg/ml) against square foot of time

Tube Extrudability. The extrudability of ointment formulations was determined in weight in grams of ointment extruded in 10 s when a certain amount of force was applied. Extrudability data were expressed as the percentage of the amount of ointment extruded from a tube in 10 s in respect to the total amount of ointment contained. The quantity in percentage of the PF ointment extruded from the tube was determined as follows (22):

$$\text{Extrudability}(\%) = \frac{\text{Amount of ointment extruded from tube}}{\text{Total amount of ointment in the tube}} \times 100$$

Stability Testing

Stability Evaluation in Simulated Wound Fluid. Simulated wound fluid (SWF) was prepared by mixing the fetal bovine serum (FBS), maximum recovery diluents (MRD, 0.1% *w/v* peptone [beef protein extract]), and 0.9% *w/v* sodium chloride in equal volumes (23).

PF solutions (1 mg/ml in water) or PF ointment formulations were added to 7 ml of simulated wound fluid (final concentration 0.7 mg/ml). The samples were incubated at 34°C for 48 h.

After incubation, supernatants were collected and properly diluted in deionized water (DIW) for HPLC analysis, while the ointment sample was recovered using a spatula and the remaining PF in the ointment was extracted into MeCN. For the extraction, samples were maintained under magnetic stirring for 12 h and then MeCN was collected and filtered through a nylon filter (0.22 μm) before dilution and HPLC analysis. After incubation, the pH of the supernatant was evaluated at time zero (pH 7.4).

Storage Stability Evaluation. Studies were carried out in accordance with current ICH/CHMP guidelines (24). PF ointment formulations packaged in aluminum tubes (10 g) were tested for short-term stability at 25 ± 2°C/60% RH conditions and for accelerated stability at 40 ± 2°C/75% RH. Ointment samples were packaged *in a closed* container that mimicked a similar closed tube used for the animal study.

Stability data covered a 13-week study at 25 ± 2°C/60% RH and accelerated study at 40 ± 2°C/75% RH. Samples (n = 3) were removed at scheduled times and the PF content was analyzed by HPLC. The centrifuge test (mechanical stress) was used to evaluate the physical stability of the ointment formulation. A 200 mg of ointment was placed into a 10-ml graduated centrifuge tube and subjected to spin at 4000 rpm for 10 min at room temperature. Results for stability were recorded at time zero and 1, 4, 8, and 13 weeks for each specified storage condition. Rheological behavior and pH were also evaluated.

pH. For the pH determination, 50 ml water was added to a 100 mg ointment sample placed in a 100-ml beaker. The beaker containing the test formulation was heated for 10 min in a water bath maintained at about 45 to 55°C, cooled to room temperature, and then centrifuged at 3000 rpm for 10 min. The pH of water extract was measured using a digital-type pH meter (PlatinumLINE high-performance pH probe with a glass body, Sartorius Corporation).

Treatment in Mice

Animal Experiments. This study has been conducted in compliance with the Animal Welfare Act, the implementing Animal Welfare Regulations, and the principles of the Guide for the Care and Use of Laboratory Animals. C57/BL6 mice 15 weeks of age were purchased from Jackson Laboratory (Bar Harbor, ME). A 2 × 3-cm area was scalded using a previously validated partial-thickness burn protocol on the dorsal area of the mouse (25). Briefly, mice were shaved and depilated with Nair the day before the burn. Under anesthesia, mice were scalded in 54°C water for 20 s. The skin was blotted with room temperature water-soaked paper towels and patted dry. The burn area was tattooed and immediately covered with 0.5 g of placebo, 1, 3.5, or 6.5% pirfenidone ointment formulations. The wound and ointment were covered with a Tegaderm film and sealed with the Vetbond tissue adhesive. At 48 h after the burn, the original Tegaderm was cut out on the inside of the Vetbond seal and replaced with a second dose of the corresponding ointment formulation, covered with Tegaderm, and sealed with Vetbond. Mice were euthanized and biological samples taken at post-operative days (POD) 3, 12, or 22.

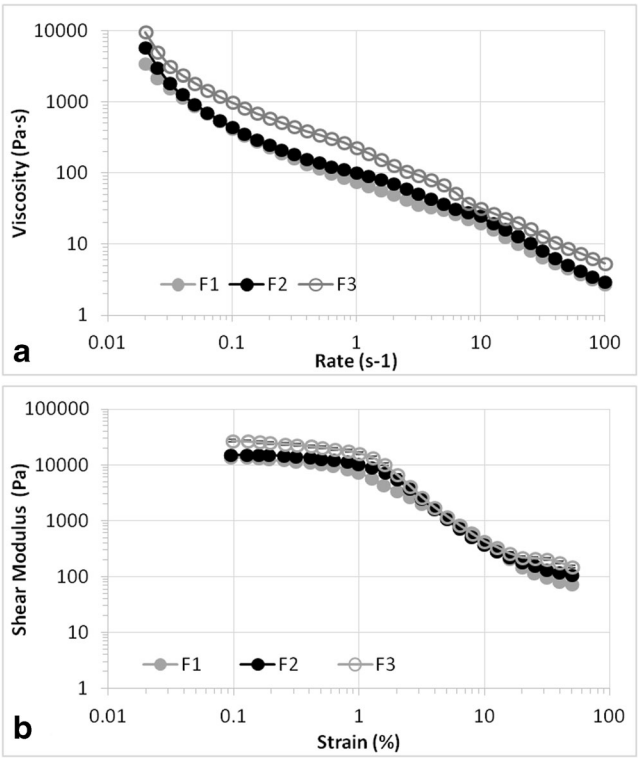

Fig. 5. Rheological characterization: shear modulus (Pa) *versus* strain (%) (**a**) and the plot of viscosity (Pa·s) *versus* shear rate (s^{-1}) (**b**)

Bio-Plex Assay. Mouse skin samples were snap-frozen upon collection. Tissues were kept at − 80°C prior to use. The skin was pulverized and homogenized in tissue lysis buffer (10 mM HEPES, 100 mM KCl, 50 mM sucrose, 1% *v/v* NP-40, 0.5% *w/v* sodium deoxycholate, pH 7.0–7.2) containing protease inhibitor mini tablets (Thermo Scientific). Samples were allowed to lyse for 4 h at 10°C with gentle rocking. Lysates were then centrifuged at 10,000 rpm for 5 min and transferred to new tubes. The lysates were evaluated for protein concentrations using a commercial BCA assay kit (Thermo Scientific). Samples were normalized to a protein concentration at 900 μg/ml and cytokines were assayed at a twofold dilution, using a Bio-Rad Pro Mouse Cytokine 23-plex magnetic bead assay kit following the procedures suggested by the manufacturer. Assay was performed using the Bio-Rad Bio-Plex 200 system and Bio-Rad Bio-Plex Pro Wash Station.

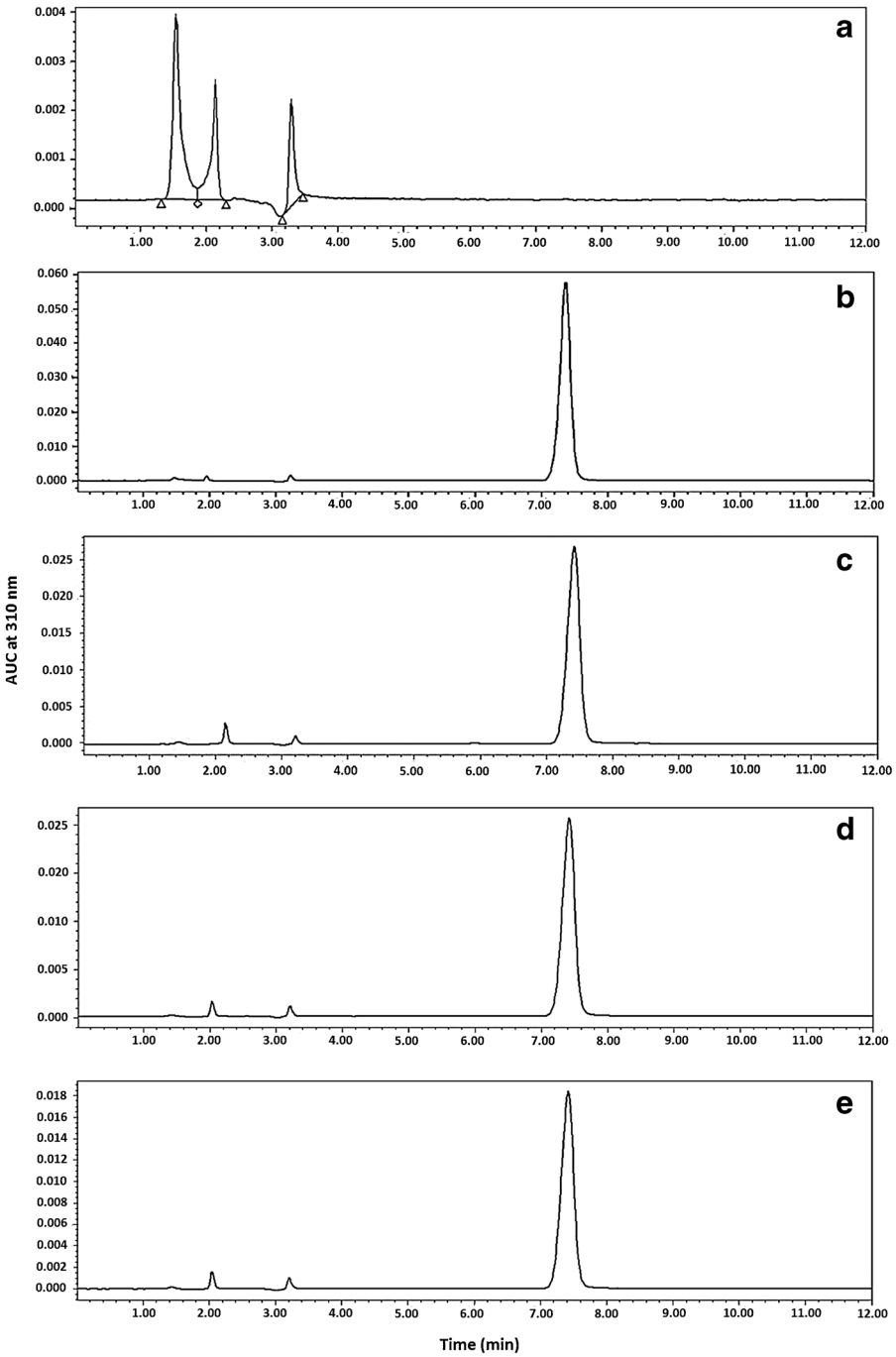

Fig. 6. HPLC chromatograms of SWF (**a**), PF incubated in SWF (0.5 mg/ml) (**b**), and PF released from ointment formulations F1 (**c**), F2 (**d**), and F3 (**e**) during incubation at 34°C for 48 h

Table IV. Physical Stability After 90-Day Storage at 40 ± 2°C/75% RH (Mean ± Sd, $n = 3$)

Formulations	Color	Clarity[a]	Homogeneity[a]	pH	Extrudability (%)	Centrifuge test[b]
F1	White	+++	+++	7.9	83.5 ± 3.5	++
F2	Off white	+++	+++	7.8	82.3 ± 1.7	++
F3	Off white	+++	+++	8.5	78.3 ± 0.9	++

[a] Key: +++ excellent, ++ very good, + good, − unsatisfactory
[a] Key: ++ no phase separation, + partial separation phase, − separation phase

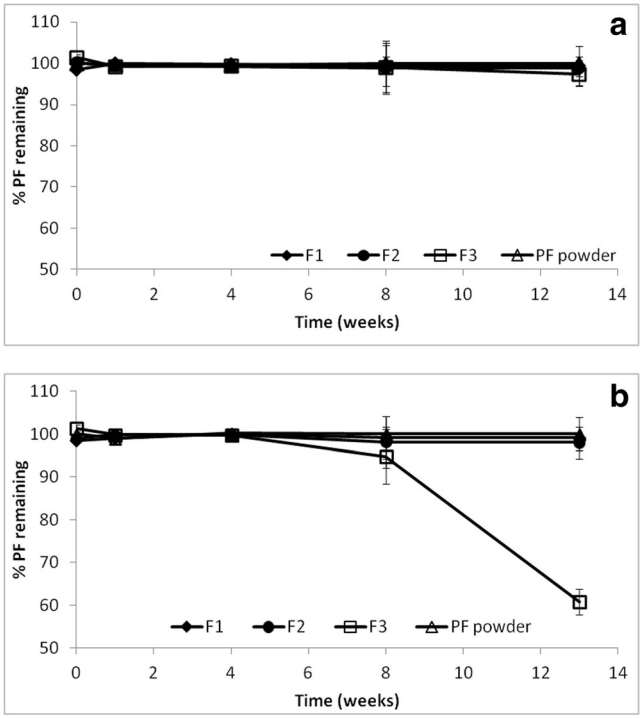

Fig. 7. Effects of temperature and relative humidity **a** 25 ± 2°C/60% RH and **b** 40 ± 2°C/75% RH (accelerated conditions) on the PF ointment formulations (F1–F3). PF powder, incubated in the same experimental conditions, was used as the control

Histology. Skin samples were fixed in formalin for 48 h. Tissues were processed in a Leica ASP6025 Tissue Processor and embedded in paraffin. Blocks were sectioned and stained with hematoxylin and eosin in a Leica Autostainer XL. The slides were automatically scanned with a Leica Aperio Versa 200 slide scanner and analyzed with the Leica ImageScope software.

RESULTS AND DISCUSSION

Preformulation Study

PF solubility in PBS at pH 7.4 was around 18 mg/ml and it did not vary with test temperature. No significant solubility variations (17 mg/ml) were observed at pH 5.0 and 6.0 suggesting that PF solubility is pH-independent. PF solubility observed in PBS at pH 5.0, 6.0, and 7.4 was consistent with the behavior of PF as a neutral compound in an aqueous environment and with the acid dissociation constant (pKa) that has been reported for PF [EMA/CHMP/115147/2011].

Although PF is slightly soluble in water (18 mg/ml), its solubility increased significantly in MeOH (46 mg/ml) and in a mixture (1:1 by volume) of H_2O:PEG (52 mg/ml).

PF solutions were stable for 28 days at different test temperatures (refrigerated conditions, 22 and 34°C) indicating the good stability of PF solutions. In the photostability study conducted at 22 and 34°C, no evidence of PF degradation during exposure to visible light for 28 days was observed (data not shown).

Quality Control Procedures

The prepared PF ointment formulations (F1–F3) (Table I) were evaluated for color, clarity, homogeneity, pH, extrudability, viscosity, and drug content (Table II). All ointments were white or off white, viscous, smooth with no grittiness, indicating uniform mixing of contents. The pH values of all ointment formulations ranged from 7.9 to 8.5, which poses no risk of irritation upon application on skin.

The drug content of all PF ointment formulations was above 98%. Uniform mixing of active with the ointment base is one of the challenging tasks in preparing topical semi-solid formulations. Drug content of F1, F2, and F3 ointment formulations (Table I) was 98.5 ± 0.9%, 98.9 ± 1.0%, and 101 ± 2.7%, respectively (Table II). The results suggested that the protocol used to prepare PF ointment formulations yielded good drug content uniformity.

Figure 3a shows *in vitro* release profiles expressed as cumulative drug release mg/ml *vs.* time (h) for PF ointment formulations (F1, F2, and F3). To facilitate optimal drug release, the percentages of ointment base, mineral oil, and PEG were varied in ointment formulations containing different doses of PF (Table I). The rate of drug release from ointment formulations increased with drug loading. After 6 h, the amount of drug released from F1 was 0.85 mg/ml whereas the amount of drug released from F2 and F3 formulations was around 3.6 mg/ml. The percentage of PF released in 24 h ranged from 53 to 66% for all the test formulations. After 48 h, F1 showed a 75% cumulative release whereas F2 and F3 showed about 90% cumulative release of PF (Fig. 3b). This should not represent an issue for the use in the animal study because the residual formulation is removed from the treatment site and replaced with a fresh ointment formulation every other day.

Among all the formulations, PF release in F1 and F2 ointment formulations was linear ($R^2 \geq 0.98$) with respect to

Table V. Degradation Constants (Day^{-1}) of PF Ointment Formulations

	F1	F2	F3
Temperature (°C/% RH)			
25 ± 2°C/60% RH	16.3×10^{-4}	16.9×10^{-4}	32.9×10^{-4}
40 ± 2°C/75% RH	30.3×10^{-4}	31.5×10^{-4}	25.4×10^{-3}
Arrhenius equation	$y = 16.967x + 4.5419$	$y = 43.429x + 4.4468$	$y = 2932.2x - 5.2569$
Ea (kJ/mol)	0.14	0.36	24.4

Ae activation energy

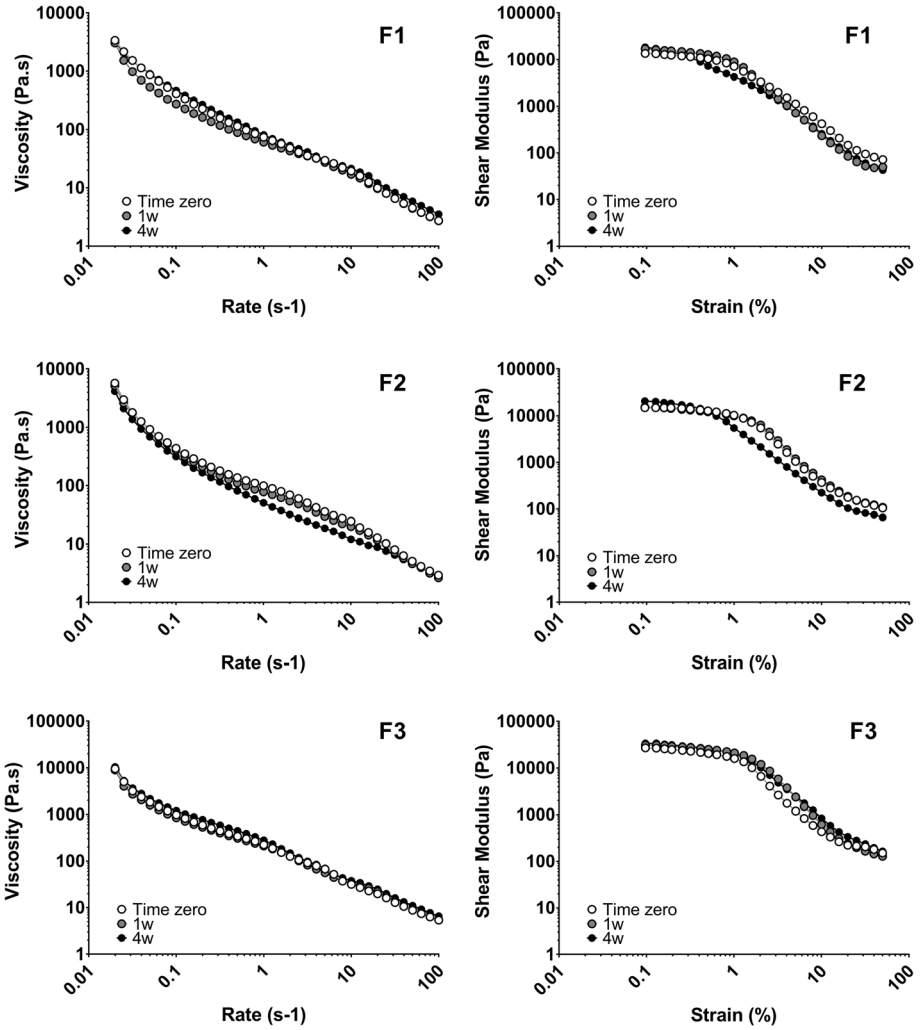

Fig. 8. Rheological characterization of the PF ointment formulations (F1, F2, and F3) for viscosity (Pa·s) *versus* strain (%) (left panel) and viscosity (Pa·s) *versus* shear rate (s^{-1}) (right panel) during the stability study at 25 ± 2°C/60% RH

the square root of time following the Higuchi model (Table III and Fig. 4c). PF release in F1 and F2 showed a higher correlation with time, as indicated by R^2, suggesting that diffusion was the primary mechanism of drug release.

In contrast, in the F3 ointment formulation, the amount of drug released was linear ($R^2 \geq 0.99$) *vs.* time (Fig. 4a), suggesting a change in the mechanism of release from that described by the Higuchi model. F3 formulation followed the zero-order model because the value of R^2 is greater in this model ($R^2 \geq 0.994$), Table III and Fig. 4a.

The dynamic oscillatory shear and shear flow are common rheological characterization protocols to characterize the stiffness and flow properties of visco-elastic materials such as ointments.

The effect of shear rate on ointment viscosity is displayed in Fig. 5a. The viscosity of prepared PF ointment formulations ranged from 3381 to 9501 Pa·s. The different viscosity values at the very low shear rate (around 0.01 s^{-1}) can be attributed to the formulation composition. The formulation with the highest PF content (F3) showed a high viscosity value, indicating F3 ointment formulation had a harder property in comparison to that of F1 and F2. Viscosity values decreased for all the ointment formulations with increasing shear rate.

Figure 5b shows shear modulus as a function of strain amplitude. It is clearly evident that as stress strain is increased the ointment formulations maintained their resistance to deform until the critical range of stresses was reached, whereupon all the formulations underwent a rapid transition from high to low modulus values. The different plateau values revealed differences among ointment formulations due to differences in composition in their resistance to deformation.

For low-strain values (around 0.1%), the shear modulus value of the F3 ointment formulation was higher than those of the F1 and F2 ointment formulations. The higher PF powder at 6.5% (F3) made the ointment stiffer. For high strain values such as 1% or above, we observed decreased shear modulus in the test formulations, suggesting that these formulations have decreases acquired a more fluid-like behavior.

The higher shear modulus for the F3 ointment formulation (1.6×10^4 Pa) could be a sign of the need for a greater applied force to squeeze the product from the tube and it could be possibly harder to apply on a vast burn area that could cause more irritation and probably pain. Differences in

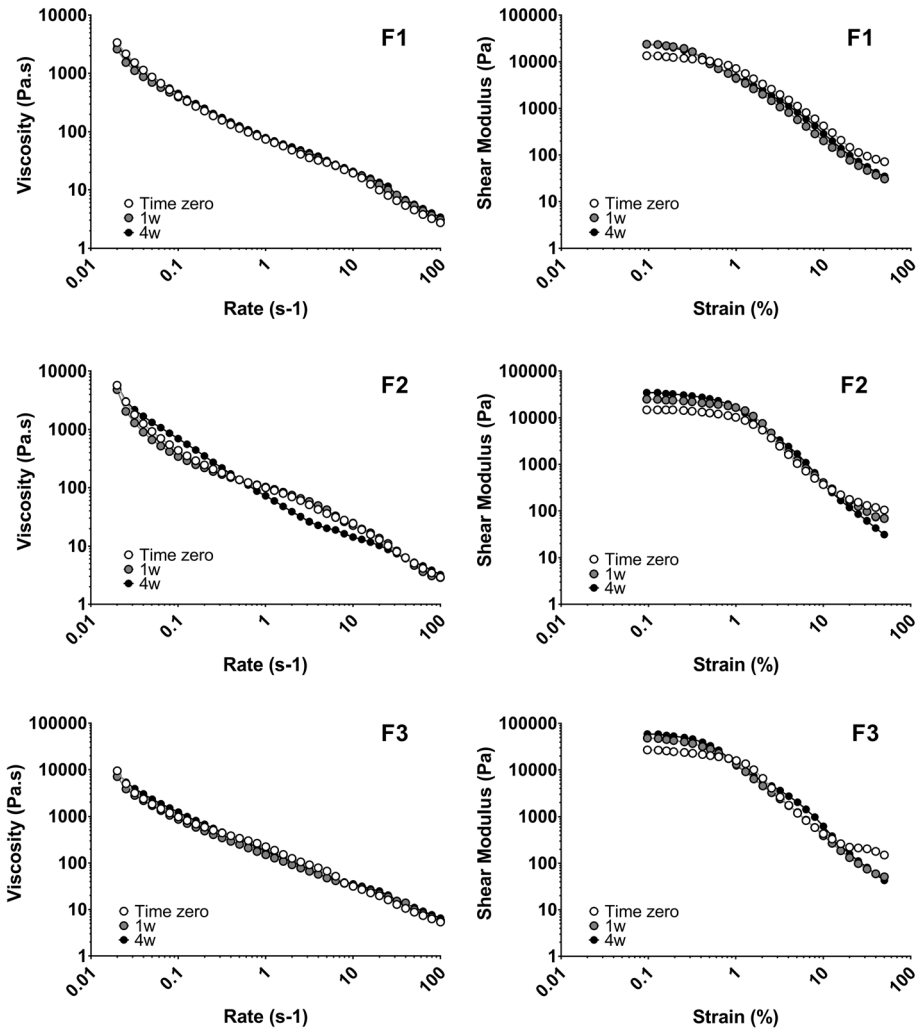

Fig. 9. Rheological characterization of the PF ointment formulations (F1, F2, and F3) for viscosity (Pa·s) *versus* strain (%) (left panel) and viscosity (Pa·s) *versus* shear rate (s^{-1}) (right panel) during the stability study at 40 ± 2°C/75% RH

rheological properties are speculated to estimate human feelings as the formulation is applied. Evaluating rheological properties may provide information that could be correlated to human feeling; therefore, differences in the rheological properties of the ointment formulations may facilitate in selecting the final formulation. The extrudability of the formulations filled into collapsible tubes (10 g) ranged from 79.9 to 83.0% (Table II).

Stability Testing

Chemical Stability Evaluation in Simulated Wound Fluid

Figure 6 shows the reversed-phase HPLC chromatograms of SWF, SWF spiked with PF, and PF released from the ointment formulations (F1, F2, and F3) after incubation for 2 days (time period required for each treatment in mouse model). HPLC analysis of PF powder spiked in SWF (Fig. 6b) and the PF ointment formulations incubated in SWF at 34°C for 48 h (Fig. 6c–e) showed no degradation products.

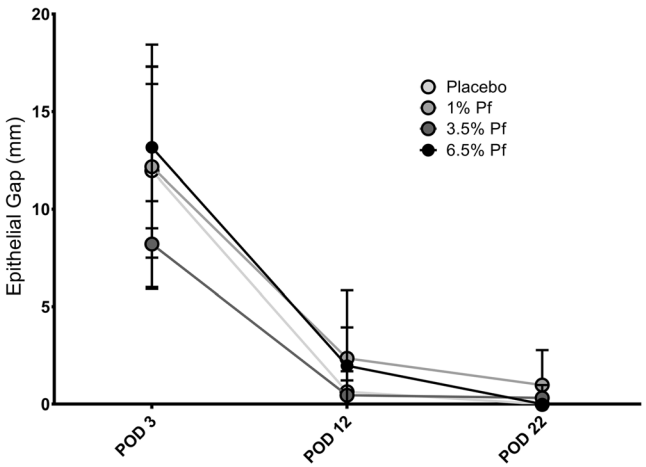

Fig. 10. Reepithelization is not significantly impacted by pirfenidone. *Epithelial gaps* were measured with the Leica ImageScope to evaluate reepithelization. There was no significant difference detected when compared to placebo (two-way ANOVA). Sham was not included as there were no gaps detected

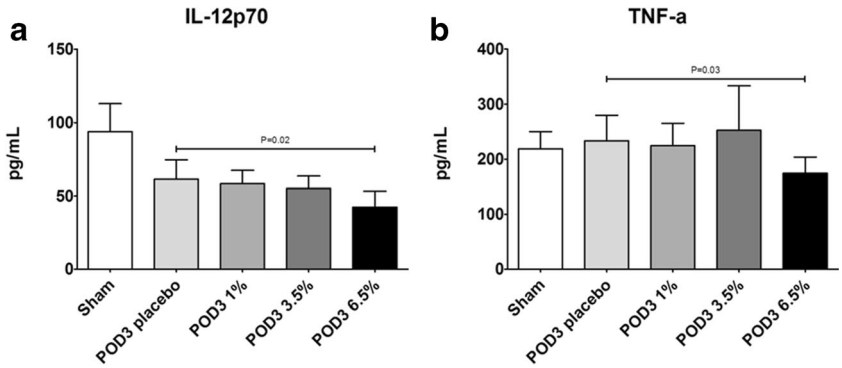

Fig. 11. PF reduces inflammatory responses in a mouse model of partial-thickness burns. Cytokines IL-12p70 (**a**) and TNFα (**b**) were measured from burn wound skin lysates using a Bio-Rad Bio-Plex system. Mice treated with 6.5% pirfenidone had significantly reduced cytokine expression at POD3 compared to placebo (*t* test)

Through 48 h, the remaining amount of the PF in the test formulations remained largely unchanged (data not shown).

Storage Stability Evaluation

The stability of PF incorporated into the F1, F2, and F3 ointment formulations was assessed at 25 ± 2°C/60% RH and in accelerated conditions at 40 ± 2°C/75% RH for 13 weeks. All the prepared PF ointment formulations were stable upon storage for 13 weeks; no changes were observed in their physical appearance, homogeneity, pH, and extrudability (Table IV).

Figure 7 shows the plots of PF remaining percentage *versus* time after incubation of PF ointment formulations at different experimental conditions. Degradation rate constants were obtained from the slope of semilog plots of the concentration *versus* time data (Table V). Temperature influenced PF degradation rate; the observed degradation rate approximately followed the first-order kinetics. The degradation constants reported in Table V demonstrated that ointment formulation containing the highest amount of PF (6.5%, F1) was less stable at 40 ± 2°C/75% RH compared to the ointment formulations F1 and F2 which contained 1 and 3.5% PF *w*/*w*, respectively. All PF ointments incubated at 25 ± 2°C/60% RH presented a good stability for 13 weeks. The relationship between temperature and rate constant is shown by Arrhenius plots (data not shown). Activation energies (Ea) derived from slope were 0.14, 0.36, and 24.38 kJ/mol for F1, F2, and F3, respectively.

In congruence with the absence of change in the visual observations, none of the formulations showed significant variations in viscosity during the stability study. The rheological behaviors of ointment formulations during storage at 25 ± 2°C/60% RH and at 40 ± 2°C/75% RH are shown in Figs. 8 and 9. According to these rheograms, all the ointment formulations stored at 25°C/60% RH showed similar rheological behavior over time (1 and 4 weeks). There were no great differences in their shear modulus *vs.* strain.

The main variation was observed for the ointment formulations F2 and F3 stored at 40 ± 2°C/75% RH. The rheogram showed a slightly increased shear modulus at 0.1% strain compared with values calculated on ointments at time zero.

Animal Experiments

Histological measurements of the wounded areas at different time intervals post burn showed no significant difference in epithelial gap (missing epidermal layer) between placebo and the treatment groups (Fig. 10). The results suggested that PF treatment did not significantly impact wound healing dynamics when treated during the inflammatory stage of wound healing after burn inductions. *Histological sections to support the measurement of the epithelial gap are included as supplemental data.*

Furthermore, treatment of partial-thickness burn wounds with 6.5% PF ointment during the inflammatory phase of a burn wound resulted in a reduced expression of pro-inflammatory cytokines IL-12p70 and TNFα (Fig. 11). This is of note considering that the mice underwent only two treatments.

TNFα and IL-12p70 are expressed during an inflammatory response by pro-inflammatory macrophages, the M1 macrophages (26). The pro-inflammatory responses are important in controlling pathogens in the wound but can have detrimental effects if left unchecked on wound healing (27). The findings suggested that the PF in ointments was anti-inflammatory, although its anti-fibrotic property to reduce burn-induced scar remains to be determined.

CONCLUSIONS

Ointment formulations containing PF at 1, 3.5, and 6.5% were successfully formulated using a mixture of ointment base, MO, and PEG. *In vitro* release results showed that the optimized ointment formulations exhibited 50% of drug release in the first 24 h and complete release after 48 h, fitting the time period required for treatment of mouse deep partial-thickness burn wounds. All the PF ointment formulations were stable physically and chemically at 25 ± 2°C/60% RH for up to 13 weeks. Animal study showed PF ointments had no adverse effects on reepithelization when used during the inflammatory stage of wound healing. The ointment formulation containing 6.5% PF (F3) caused a reduced expression of pro-inflammatory cytokines IL-12p70 and TNFα. These optimized PF hydrocarbon base ointment formulations could be a promising dosage form for topical delivery of PF in treatment of deep partial-thickness burn.

FUNDING INFORMATION

RD performed this study at the US Army Institute of Surgical Research during her sabbatical leave from the University of Pavia, Italy. Her stipend was supported by an appointment to the Postgraduate Research Participation Program at the US Army Institute of Surgical Research administered by the Oak Ridge Institute for Science and Education through an interagency agreement between the US Department of Energy and US Army Medical Research and Materiel Command (USAMRMC). This work was supported in part through the Congressionally Directed Medical Research Programs, USAMRMC W81XWH-15-2-0083, and the Naval Medical Research Center's Advanced Medical Development program (MIPR N3239815MHX040).

COMPLIANCE WITH ETHICAL STANDARDS

This study has been conducted in compliance with the Animal Welfare Act, the implementing Animal Welfare Regulations, and the principles of the Guide for the Care and Use of Laboratory Animals.

Conflict of Interest The authors declare that they have no conflict of interest.

Disclosure The opinions or assertions contained herein are the private views of the authors and are not to be construed as official or as reflecting the views of the Department of the Army or the Department of Defense.

REFERENCES

1. Tredget EE, Levi B, Donelan MB. Biology and principles of scar management and burn reconstruction. Surg Clin North Am. 2014;94(4):793–815.
2. Qian L-W, Fourcaudot AB, Yamane K, You T, Chan RK, Leung KP. Exacerbated and prolonged inflammation impairs wound healing and increases scarring. Wound Repair Regen. 2016;24(1):26–34.
3. Penn JW, Grobbelaar AO, Rolfe KJ. The role of the TGF-β family in wound healing, burns and scarring: a review. Int J Burns Trauma. 2012;2(1):18–28.
4. Karagoz H, Sever C, Bayram Y, Sahin C, Kulahci Y, Ulkur E. A review of the prevention and treatment of hypertrophic scars: part I clinical aspects. Arch Clin Exp Surg (ACES). 2012;1(4):237–48.
5. Aarabi S, Longaker MT, Gurtner GC. Hypertrophic scar formation following burns and trauma: new approaches to treatment. PLoS Med. 2007;4(9):1464–70.
6. Wasiak J, Cleland H, Campbell F, Spinks A. Dressings for superficial and partial thickness burns. Cochrane Database Syst Rev. 2013;3:1–85.
7. J Schaefer C, W Ruhrmund D, Pan L, Seiwert S, Kossen K. Antifibrotic activities of pirfenidone in animal models. Eur Respir Rev. 2011;20(120):85–97.
8. Veras-Castillo ER, Cardenas-Camarena L, Lyra-Gonzalez I, Munoz-Valle JF, Lucano-Landeros S, Guerrerosantos J, et al. Controlled clinical trial with pirfenidone in the treatment of breast capsular contracture: association of TGF-beta polymorphisms. Ann Plast Surg. 2013;70(1):16–22.
9. Armendariz-Borunda J, Lyra-Gonzalez I, Medina-Preciado D, Gonzalez-Garcia I, Martinez-Fong D, Miranda RA, et al. A controlled clinical trial with pirfenidone in the treatment of pathological skin scarring caused by burns in pediatric patients. Ann Plast Surg. 2012;68(1):22–8.
10. NIH U.S. National Library of Medicine - ClinicalTrials.gov [cited 12.14.2017]. Available from: https://clinicaltrials.gov/ct2/results?term=pirfenidone+AND+fibrosis&Search=Search.
11. Rowan MP, Cancio LC, Elster EA, Burmeister DM, Rose LF, Natesan S, et al. Burn wound healing and treatment: review and advancements. Crit Care. 2015;19:1–12.
12. Hall CL, Wells AR, Leung KP. Pirfenidone reduces profibrotic responses in human dermal myofibroblasts, in vitro. Lab Investig. 2018. https://doi.org/10.1038/s41374-017-0014-3
13. Moran N. p38 kinase inhibitor approved for idiopathic pulmonary fibrosis. Nat Biotech. 2011;29(4):301.
14. Furukawa F, Matsuzaki K, Mori S, Tahashi Y, Yoshida K, Sugano Y, et al. p38 MAPK mediates fibrogenic signal through smad3 phosphorylation in rat myofibroblasts. Hepatology. 2003;38(4):879–89.
15. Rodríguez-Castellanos M, Tlacuilo-Parra A, Sánchez-Enríquez S, Vélez-Gómez E, Guevara-Gutiérrez E. Pirfenidone gel in patients with localized scleroderma: a phase II study. Arthritis Res Ther. 2014;16(510):1–8.
16. Giri SN, Margolin SB. Effects of topical application of pirfenidone ointment on thermoplasty-induced acute lameness in a double-blind and acute and chronic lameness of musculoskeletal origin in an open multi-centered field trial in horses. Res Commun Mol Pathol Pharmacol. 2005;117-118:47–63.
17. Parmar V, Desai SB, Vaja T. RP-HPLC and UV spectrophotometric methods for estimation of pirfenidone in pharmaceutical formulations. Indian J Pharm Sci. 2014;76:225–30.
18. Thorat S, P Padmane S, R Tajne M, M Ittadwar A. Development and validation of simple, rapid and sensitive UV, HPLC and HPTLC methods for the estimation of pirfenidone in tablet dosage form. J Chil Chem Soc. 2016;61(2):2978–81.
19. Babu Bodempudi S, Babur R, Srinivasa Reddy K. Development and substantiation of a RP-HPLC method for monitoring of impurities in pirfenidone drug substance. Am J Anal Chem. 2015;06:1019–29.
20. Salerno C, Carlucci AM, Bregni C. Study of in vitro drug release and percutaneous absorption of fluconazole from topical dosage forms. AAPS PharmSciTech. 2010;11(2):986–92.
21. Lokhandwala H, Deshpande A, Deshpande S. Kinetic modeling and dissolution profiles comparison: an overview. Int J Pharm. 2013;4(1):728–38.
22. Rajesh Asija SP, Sangeeta Asija, Sandeep Kataria Formulation and evaluation of herbal ointment of Murraya koenigii. Int J Pharm Res Bio-Sci 2015;4(3):433–443.
23. Said J, Dodoo CC, Walker M, Parsons D, Stapleton P, Beezer AE, et al. An in vitro test of the efficacy of silver-containing wound dressings against Staphylococcus aureus and Pseudomonas aeruginosa in simulated wound fluid. Int J Pharm. 2014;462(1):123–8.
24. ICH Topic Q 1 A (R2) Stability testing of new drug substances and products. Note for guidance on stability testing: stability testing of new drug substances and products (CPMP/ICH/2736/99) [Internet]. [cited 12.14.2017]. Available from: http://www.ich.org/products/guidelines/quality/quality-single/article/stability-testing-of-new-drug-substances-and-products.html.
25. Medina JL, FFA, Sebastian EA, Shankar R., Brown AW and, KP L Standardization of deep partial-thickness scald burns in C57BL/6 mice. Int J Burn Trauma. 2018;(8)2
26. Zheng X-F, Hong Y-X, Feng G-J, Zhang G-F, Rogers H, Lewis MAO, et al. Lipopolysaccharide-induced M2 to M1 macrophage transformation for IL-12p70 production is blocked by Candida albicans mediated up-regulation of EBI3 expression. PLoS One. 2013;8(5):1–10.
27. Ashcroft GS, Jeong M-J, Ashworth JJ, Hardman M, Jin W, Moutsopoulos N, et al. Tumor necrosis factor-alpha (TNF-α) is a therapeutic target for impaired cutaneous wound healing. Wound Repair Regen. 2012;20(1):38–49.